The electric field of synchrotron radiation

BY J. H. HANNAY AND M. R. JEFFREY

*H.H. Wills Physics Laboratory, University of Bristol, Tyndall Avenue,
Bristol BS8 1TL, UK*

A point charge moving uniformly around a circle produces an electric field pattern which co-rotates with it, constituting, for relativistic motion, synchrotron radiation. Surprisingly perhaps, the wealth of knowledge on synchrotron radiation does not seem to include *explicit* knowledge of the field itself, and of the consequent field lines. As with any relativistic motion, there is an obstruction to writing an explicit formula for the field; evaluation of the retarded time requires solving an implicit equation. However, as the relativistic limit is approached the field grows very strong in a very confined ribbon region shaped like a spiral watch spring. Here, the field *can* be written as an explicit scaling, or universal similarity, formula, which is our main result. From it the field lines can be derived analytically. In terms of scaled coordinates along the directions of the length, width and thickness of the ribbon, they twist in two side-by-side bundles in 'bipolar' cylinder surfaces, mirror symmetric about the orbit plane.

Keywords: electric field; synchotron radiation; scaling theory

1. Introduction

A great deal is known (Jackson 1999; Duke 2000) about synchrotron radiation, namely the radiation from a point charge moving uniformly in a circle at relativistic speed βc. The pattern of electric and magnetic fields rotates rigidly with the charge. Surprisingly perhaps, all this theoretical and experimental understanding seems not to have required explicit knowledge of the field itself (in the 'time domain' as it is sometimes called), and of the geometry of its field lines in space. Conventional analysis concentrates instead on the most practically useful functionals of the field such as its temporal Fourier transform (frequency spectrum) and the angular power distribution at large range. To obtain the field itself one must start further back. As is the usual practice, we shall concentrate on the electric field because the magnetic field is naturally obtained from it (and also because the magnetic field structure is dull in comparison with the electric, as we explain in the concluding remarks).

There is an obstruction to writing an explicit formula for the fields from any moving charge; the expression for $\boldsymbol{E}$ (and $\boldsymbol{B}$) involves the retarded position. To locate this requires solving an implicit (i.e. transcendendal) equation of the form $\sin\theta \propto \theta^2 + \text{const.}\,\theta + \text{const.}$ This is little hindrance to numerical computation by iteration (though high accuracy is required relativistically, and we have used it to check our results numerically). Nevertheless, the lack of an explicit formula for the field, especially in the synchrotron case where it is constant in time in the
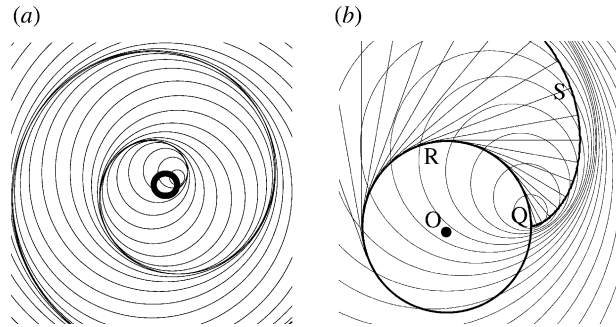
Figure 1. (*a*) For a hypothetical point charge circulating at the speed of light the nested spheres of constant retardation generate a curve as their caustic; the unwrap spiral in the orbit plane formed by a geometrical construction shown on the right. (*b*) For a charge circulating at close to the speed of light the nested spheres of constant retardation crowd up dramatically just outside the unwrap spiral. This spiral is generated by a hypothetical taut string with endpoint S unwrapping from the bold ring (the orbit) centre O. Before unwrapping, the string end lies at Q, the present position of the charge.

co-rotating coordinates, is disappointing. It also effectively prevents any analytical attempt to describe the field lines, in other words to 'integrate' the flow field. The adverse consequences of implicitness are also felt in the conventional analysis of functionals of the field, forcing approximation.

One might hope that invoking the relativistic limit, which is closely approximated in the synchrotron, would simplify matters, and it does in the following respects. The field becomes stronger and stronger in a smaller and smaller region near a particular curve in space. Elsewhere, the field attains a finite value in the limit, the field lines being almost complete circles. Though simple, the implicit step in the algebraic representation persists as an obstruction (to finding which circle), and we shall have little further to say about the finite field. The high-field region, on the other hand, where the field grows stronger as $\beta \rightarrow 1$, is sufficiently confined that the obstruction of implicitness can be circumvented and the field does have a simple explicit scaling, or universal similarity, expression to be derived. It should be mentioned that an asymptotic scaling relationship for the frequency power spectrum of synchrotron radiation was noted in 1981 by Risley *et al.* (1981). For us, seeking the field itself, the problem is largely geometrical and some preparatory geometry is needed.

2. Preparatory geometry

The involute curve or 'unwrap spiral', of a circle, is obtained by imagining the past trajectory of the circulating charge to be a thread wound up around a post (figure 1). The end of the thread is where the charge is now (Q). Unwrap the thread from the post, round and round in the same plane, keeping it taut. The locus of the thread end S defines the unwrap spiral. It is in a narrow region asymptotically close to the unwrap spiral that the electric field diverges in the relativistic limit.

An associated geometrical intensification underlies that of the field. Space is filled with nested 'spheres of constant retardation'. Each is centred on some point R on the orbit circle lying at some angle θ backwards around the orbit circle from

the present position of the charge Q. R represents the common retarded position of the charge for all field points on its sphere. If the orbit circle has radius a, the unwrapped length of thread RS equals the arc length, $a\theta$, and S represents the 'extrapolated' position of the charge; where it would be now if it had been released from the circle orbit at R, and drifted at constant velocity. The radius of the sphere of constant retardation centred on R is $a\theta/\beta$.

For $\beta=1$ (hypothetically), successive nested spheres of constant retardation touch their neighbours at the points S of the unwrap spiral curve, that is, the unwrap spiral is the 'caustic' of the spheres, and the field is infinite there. For β close to 1 the spheres do not touch but are very crowded up just outside the unwrap spiral, and the region of dense crowding is a ribbon (length $\gg$ width $\gg$ thickness) wound like a spiral watch spring. The cross-section of the watch spring ribbon is not flat but arched (to match the local sphere surface). In this densely crowded region the field is strongest. The location can be specified more precisely with the help of a suitably defined orthogonal coordinate system in three dimensions.

Let the orbit plane be called horizontal and denote height above it by the coordinate z. Vertical half planes tangent to the orbit circle supply perpendicular cross-sections across the unwrap spiral (the half planes having a vertical boundary edge through the tangency point). The cross-section half planes are to be labelled by the angle θ_0 of their tangency point around the orbit circle. It is important to distinguish this coordinate θ_0, constant on half planes, from the variable θ, constant on retardation spheres. It will turn out that in the high-field region the values of θ_0 and θ differ only slightly, but crucially.

On the cross-section half planes the coordinates are to be ordinary Cartesian ones x, and the height z. To make an orthogonal coordinate system together with θ_0, the origin of x needs to be on the unwrap spiral (since, the spiral intersects the half plane perpendicularly). In other words, x and z are coordinates marked on a rigid vertical plane rolling, without slipping, on the orbit circle, and having $x=z=0$ at Q. We shall not be troubled by the lack of coordinates 'inside' the orbit circle which the half plane never accesses (being tangent to it), nor by the multiple covering as the half plane sweeps through more than one turn.

The locus of special points for which $\theta=\theta_0$ is the family of semicircles, radius $a\theta_0/\beta$, whose retarded points do exactly lie at the tangency points of their half planes. On each semicircle, there is a small central arc 'outside' S, that is, with $x>0$. It is the family of these small arcs that will generate the arched sectioned ribbon region of high field (figure 2). The depth of the arch is $a\theta_0(\beta^{-1}-1)$, which means, with $\gamma=1/\sqrt{1-\beta^2}$, that it is proportional to $1/\gamma^2$ relativistically. In consequence, the span of the arch perpendicular to the orbit plane is proportional to $1/\gamma$. This is the well-known 'beam width' of synchrotron radiation. It will emerge later (after equation (4.9)) that the thickness of the high-field ribbon region is proportional to $1/\gamma^3$. This important $\sim 1/\gamma^3$ thickness has also been more or less known all through the synchrotron literature; for example, a heuristic argument is given in Duke (2000, eq. 14.49), and a geometric calculation of a field feature is given in Tsien (1972; Fig. 7), to be mentioned later (after equation (4.9)). It is also inherent in the standard spectral calculation (Jackson 1999; Duke 2000) of synchrotron radiation.

Having zero divergence (though not zero curl) the electric field is legitimately described in terms of unending field lines from the charge, whose flux density supplies the field magnitude. In the strong field region described, these field lines
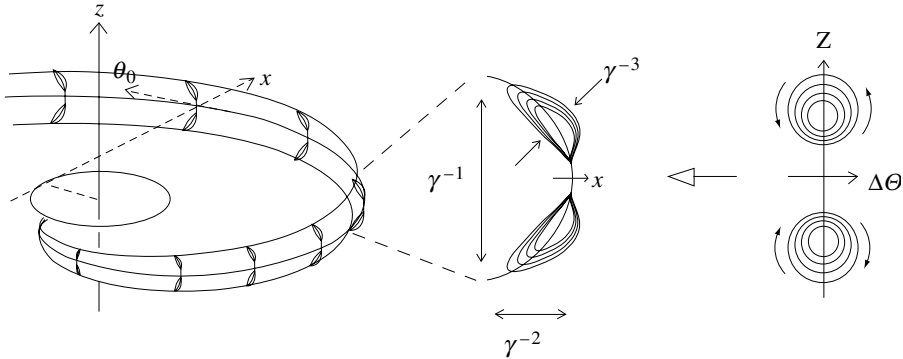
Figure 2. Oblique view of the orbit (radius a), and the unwrap spiral. Along the spiral a ribbon-like region of high electric field (for $\beta = 0.99$) is shown. The ribbon is very narrow, relativistically, with width $\sim 1/\gamma$, arch-depth $\sim 1/\gamma^2$, and thickness $\sim 1/\gamma^3$. Its cross-section in scaled coordinates $(\Delta\Theta, Z)$ consists of sets of bipolar circles whose flow direction is shown.

will be shown to form two, side by side, oppositely twisted bundles, mirror symmetric about the orbit plane. The cross-section of each of the two bundles is strongly squashed to form (half) the arch shape. The field lines, while twisting, proceed along the spiral (though not everywhere monotonically). The starting point for this analysis is the standard set of formulas for the field (figure 2).

3. The standard field formulas

The electric field (and thence the magnetic one) from a point charge in general motion can be written either (Jackson 1999) in the Heaviside–Feynman form, or the more conventional velocity–acceleration form (Jackson 1999; Duke 2000), which we use here. The formula expresses $\boldsymbol{E}$ as $\boldsymbol{E} = \boldsymbol{E}_{\text{vel}} + \boldsymbol{E}_{\text{acc}}$, where $\boldsymbol{E}_{\text{vel}}$ depends only on the velocity, not the acceleration, at the retarded time, while $\boldsymbol{E}_{\text{acc}}$ is proportional to the acceleration. For our case of uniform circular motion, the field $\boldsymbol{E}$ is constant in time at a fixed position P in the coordinates co-rotating with the charge. It can be expressed in terms of the retarded position R (with its associated extrapolated position S), which depends on P, and the circle centre O. If the charge has velocity βc, the formulas for $\boldsymbol{E}$ (and $\boldsymbol{B}$) are

$$\boldsymbol{E} = \boldsymbol{E}_{\text{vel}} + \boldsymbol{E}_{\text{acc}}, \tag{3.1}$$

$$\boldsymbol{E}_{\text{acc}} = (q/4\pi\varepsilon_0)(\beta^2/a^2)\underline{\text{RP}} \wedge (\underline{\text{SP}} \wedge \underline{\text{RO}})\text{RP}^3/(\underline{\text{SP}} \cdot \underline{\text{RP}})^3, \tag{3.2}$$

$$\boldsymbol{E}_{\text{vel}} = (q/4\pi\varepsilon_0)(1/\gamma^2)\underline{\text{SP}}\,\text{RP}^3/(\underline{\text{SP}} \cdot \underline{\text{RP}})^3, \tag{3.3}$$

$$\boldsymbol{B} = \underline{\text{RP}} \wedge \boldsymbol{E}/c\text{RP}. \tag{3.4}$$

Evidently $\boldsymbol{E}_{\text{acc}}$ lies everywhere tangent to the nested spheres of constant retardation (perpendicular to $\underline{\text{RP}}$). Indeed, the lines of $\boldsymbol{E}_{\text{acc}}$ are circles (figure 3), all of them on any given sphere passing through the two null points U_1 and U_2 where $\boldsymbol{E}_{\text{acc}}$ is zero on the sphere (the chord U_1, U_2 has midpoint S and is parallel
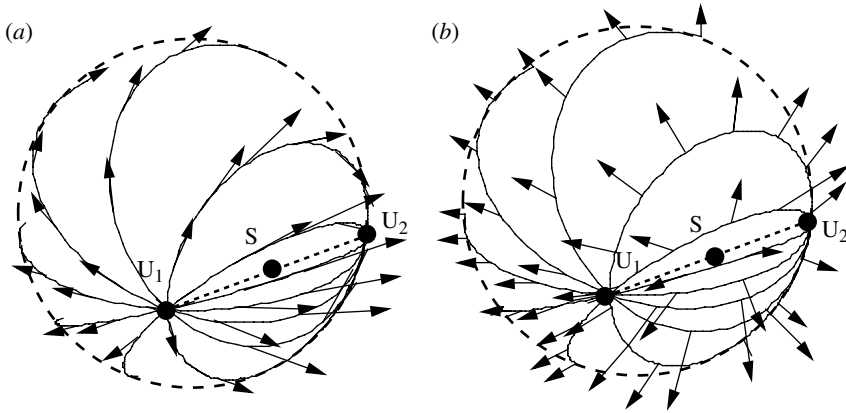
Figure 3. Field geometry. (*a*) The acceleration field $\boldsymbol{E}_{\mathrm{acc}}$ is everywhere tangent to arcs on the spheres of constant retardation, centre R, along circle arcs from the point U_1 and the point U_2, at each of which the field vanishes. U_1 to U_2 lie in the orbit plane with the midpoint of the chord between them at S. (*b*) The velocity field $\boldsymbol{E}_{\mathrm{vel}}$ over the same surface points everywhere radially outward from the point S. Both pictures are for $\beta = 0.8$.

to OR). $\boldsymbol{E}_{\mathrm{vel}}$ on the other hand pierces the spheres, directed radially out from S (a different S, though, for each sphere). Using the retardation condition $\beta\mathrm{RP} = \mathrm{RS}$, the quantity in the denominator $\underline{\mathrm{SP}} \cdot \underline{\mathrm{RP}} = (\underline{\mathrm{RP}} - \underline{\mathrm{RS}}) \cdot \underline{\mathrm{RP}}$, can only be zero in the extreme relativistic limit and even then only if P=S. Thus, in this limit $\boldsymbol{E}_{\mathrm{acc}}$ is finite, not infinite, except on the unwrap spiral, and by the same reasoning $\boldsymbol{E}_{\mathrm{vel}}$ is zero because of the infinite γ factor. Approaching the limit, then, $\boldsymbol{E}_{\mathrm{acc}}$ dominates almost everywhere, both outside and inside the high-field region of interest. However, inside the high-field region the components of $\boldsymbol{E}_{\mathrm{acc}}$ and $\boldsymbol{E}_{\mathrm{vel}}$ in the 'crowded-up' x direction (of the retardation spheres) are comparable, and $\boldsymbol{E}_{\mathrm{vel}}$ must be retained for the correct connectivity of the field lines.

4. The scaling analysis

The scaling formula for the electric field as the relativistic limit is approached derives from appropriate Taylor expansion of the numerator and denominator of the formulas (3.1–3.3), to be carried out shortly. It is natural to fix the cross-section half plane ($\theta_0 = $ constant) and expand jointly in the coordinates in that plane as well as in the quantity $(1 - \beta)$ measuring deviation from the relativistic extreme. Actually, although the coordinate z is acceptable as an expansion variable, the coordinate x is not good directly, for the reason given below equation (4.8) (roughly speaking, because of the crowding up of spheres in this direction). Instead the expansion needs to be in the (uncrowded) variable labelling the spheres, namely the polar angle coordinate θ of the retarded position R. The criterion for the leading terms in a multi-variable expansion is Newton's polyhedron convex hull construction in index space, though for us it is simple enough to be obvious anyway.

Given a field point P with coordinates (x, θ_0, z), the associated retarded position R, at angle θ backwards around the orbit circle, is only expressible

implicitly in terms of P. Requiring that RP equals $a\theta/\beta$ gives

$$[a\sin(\theta-\theta_0) + a\theta_0 + x]^2 + a^2[1 - \cos(\theta-\theta_0)]^2 + z^2 = (a\theta/\beta)^2. \qquad (4.1)$$

Thus, θ is an implicit function of (x, θ_0, z) though x is an explicit function of θ_0, z and θ. In particular for $\theta = \theta_0$, the (appropriate) solution for x is $x_0 = -a\theta_0 + \sqrt{(a\theta_0/\beta)^2 - z^2}$. Setting $\Delta x = x - x_0$ and $\Delta \theta = \theta - \theta_0$ and expanding the equation (4.1) jointly in $(1-\beta)$ and $\Delta\theta_0$ gives the cubic equation

$$\Delta x/a = \frac{1}{6}\Delta\theta^3 + (1 - \beta + \frac{1}{2}(z/a\theta_0)^2)\Delta\theta. \qquad (4.2)$$

The cubic has a single real root,

$$\Delta\theta = [\cdot]^{1/3} - 2(1 - \beta + \frac{1}{2}(z/a\theta_0)^2)[\cdot]^{-1/3}, \qquad (4.3)$$

where

$$[\cdot] = [3\Delta x/a + \sqrt{8(1 - \beta + \frac{1}{2}(z/a\theta_0)^2)^3 + 9(\Delta x/a)^2}], \qquad (4.4)$$

the square and cube roots being real and positive. Though now explicit by virtue of the expansion, this solution is non-analytic, involving these roots, and this is the mathematical obstruction to a direct expansion in x.

For the expansion of the field we calculate three components, an 'x' one which requires further comment, and straightforward y and z ones, where y is perpendicular to the x, z plane. In fact $(a\theta_0 + x)\nabla\theta_0$ is the unit vector in the y direction, and the $x\nabla\theta_0$ part of this is negligible. The 'x', y and z components to be calculated are specifically: $\boldsymbol{E}\cdot a\theta_0\nabla\Delta\theta$, $\boldsymbol{E}\cdot a\theta_0\nabla\theta_0$, $\boldsymbol{E}\cdot\nabla z$, and all three will turn out to be of the same order, γ^4 relativistically. The last two are straightforward field components, the multiplying vectors being unit vectors (relativistically). The x component of $\boldsymbol{E}$ is much smaller ($\boldsymbol{E}\cdot\nabla x$ is of order γ^3 and $\boldsymbol{E}\cdot\nabla\Delta x$ is of order γ^2), relativistically, but is nonetheless vital for finding the field lines. Its multiplying vector, the gradient $a\theta_0\nabla\Delta\theta$, is large in compensation, involving $\Delta\theta$ rather than x or Δx to conform with the choice of expansion coordinate. Its direction, though not exactly in the x direction, is asymptotically so as $\beta \to 1$. For the y and z components it suffices to use $\boldsymbol{E} \approx \boldsymbol{E}_{\text{acc}}$, since $\boldsymbol{E}_{\text{vel}}$ is of order γ^2 only, but for the 'x' one both parts are required because $\boldsymbol{E}_{\text{acc}}$ is nearly perpendicular to $\nabla\Delta\theta$.

All the three field components sought share the same denominator $(\underline{\text{SP}}\cdot\underline{\text{RP}})^3$ so we start by finding the expansion of $\underline{\text{SP}}\cdot\underline{\text{RP}}$.

$$\underline{\text{SP}}\cdot\underline{\text{RP}} = x(x + a\theta_0 + a\sin\Delta\theta) + z^2. \qquad (4.5)$$

With x supplied by the solution of equation (4.1) this gives, on expansion

$$\underline{\text{SP}}\cdot\underline{\text{RP}} \approx a^2\theta_0^2[(1-\beta) + \frac{1}{2}\Delta\theta^2 + \frac{1}{2}(z/a\theta_0)^2]. \qquad (4.6)$$

Next, we expand the numerators of the field components. The common factor $\{q\text{RP}^3/4\pi\varepsilon_0(\underline{\text{SP}}\cdot\underline{\text{RP}})^3\}$ will be shortened to [*]. We treat the x component last, since it is the most subtle.

Using $a\theta_0\boldsymbol{\nabla}\theta_0 \approx \theta_0|\boldsymbol{\nabla}\theta_0|\underline{\mathrm{OR}} \approx \underline{\mathrm{OR}}/a$ (the first equality is not exact because R lies at angle θ, not θ_0, around the orbit circle; the second because the exact relation is $(a\theta_0 + x)|\boldsymbol{\nabla}\theta_0| = 1$, as stated above), we have, for the y component,

$$\boldsymbol{E}\cdot a\theta_0\boldsymbol{\nabla}\theta_0 \approx \boldsymbol{E}_{\mathrm{acc}}\cdot a\theta_0\boldsymbol{\nabla}\theta_0 \approx [^*](\beta^2/a^2)(1/a)\underline{\mathrm{OR}}\cdot(\underline{\mathrm{RP}}\wedge(\underline{\mathrm{SP}}\wedge\underline{\mathrm{RO}})) \quad (4.7)$$

$$\begin{aligned} = [^*](\beta^2/a^3)[(\underline{\mathrm{OR}}\cdot\underline{\mathrm{SP}})(\underline{\mathrm{RP}}\cdot\underline{\mathrm{RO}}) \\ -(\underline{\mathrm{OR}}\cdot\underline{\mathrm{RO}})(\underline{\mathrm{RP}}\cdot\underline{\mathrm{SP}})] \end{aligned} \quad (4.8)$$

$$\approx [^*]a\theta_0^2[(1-\beta) + \frac{1}{2}(z/a\theta_0)^2 - \frac{1}{2}\Delta\theta^2]. \quad (4.9)$$

For $z=0$ the two locations where this component is zero, namely $\Delta\theta = \pm\sqrt{2(1-\beta)}$ generate, as θ_0 varies, a pair of curves in space running side by side outside the unwrap spiral. Their spatial separation is, from equation (4.2), a constant in space: $2\Delta x = 8\sqrt{2(1-\beta)^3}a/3$. The curves are the (expansion approximation to the) loci in space of the points U_1 and U_2 (figure 3) on successive spheres. Actually the U_1 and U_2 arms of this locus join together near the charge, forming a single curved U-shape, whose geometry was well described by Tsien (1972, fig. 7).

Next the z component,

$$\boldsymbol{E}\cdot\boldsymbol{\nabla}z \approx \boldsymbol{E}_{\mathrm{acc}}\cdot\boldsymbol{\nabla}z \approx [^*](\beta^2/a^2)a\theta_0^2\Delta\theta z/a\theta_0. \quad (4.10)$$

Finally, the 'x' component can be found using $\boldsymbol{E}_{\mathrm{acc}}\cdot\boldsymbol{\nabla}\theta=0$, since $\boldsymbol{E}_{\mathrm{acc}}$ is tangent to the sphere of constant retardation.

$$\boldsymbol{E}\cdot a\theta_0\boldsymbol{\nabla}\Delta\theta = \boldsymbol{E}_{\mathrm{vel}}\cdot a\theta_0\boldsymbol{\nabla}\theta - \boldsymbol{E}\cdot a\theta_0\boldsymbol{\nabla}\theta_0. \quad (4.11)$$

The last term was expanded in equation (4.7) above. The first can be evaluated exactly using $a|\boldsymbol{\nabla}\theta| = \beta\mathrm{RP}^2/\underline{\mathrm{SP}}\cdot\underline{\mathrm{RP}}$. (This formula follows from the geometry of adjacent nested spheres: the gap at P between the spheres θ and $\theta+\mathrm{d}\theta$ is $a\,\mathrm{d}\theta(1-\cos\angle\mathrm{SRP})/\beta = a\,\mathrm{d}\theta\underline{\mathrm{SP}}\cdot\underline{\mathrm{RP}}/\beta\mathrm{RP}^2$.)

$$\begin{aligned} \boldsymbol{E}_{\mathrm{vel}}\cdot a\theta_0\boldsymbol{\nabla}\theta &= [^*](1/\gamma^2)\theta_0(\beta\mathrm{RP}^2/\underline{\mathrm{SP}}\cdot\underline{\mathrm{RP}})(\underline{\mathrm{SP}}\cdot\underline{\mathrm{RP}})/\mathrm{RP} \\ &= [^*](1/\gamma^2)\beta\theta_0\mathrm{RP}. \end{aligned} \quad (4.12)$$

This can then be combined with the last term from equation (4.11) above and expanded, using $1/\gamma^2 \approx 2(1-\beta)$,

$$\boldsymbol{E}\cdot a\theta_0\boldsymbol{\nabla}\Delta\theta \approx [^*]a\theta_0^2\left[2(1-\beta) - \left[(1-\beta) - \frac{1}{2}\Delta\theta^2 + \frac{1}{2}(z/a\theta_0)^2\right]\right] \quad (4.13)$$

$$= [^*]a\theta_0^2\left[(1-\beta) + \frac{1}{2}\Delta\theta^2 - \frac{1}{2}(z/a\theta_0)^2\right]. \quad (4.14)$$

We now summarize these results. The dot product of the field $\boldsymbol{E}(x, \theta_0, z)$ with three basis vectors is supplied, the vectors having, relativistically, the directions of the orthogonal coordinates (x, θ_0, z). All have the same order γ^4, and the latter two directly represent field components, since the vectors are unit vectors (relativistically). The first component is much smaller (the multiplying vector

being much larger than a unit vector) but is nonetheless essential for the correct specification of the field lines.

$$\boldsymbol{E}\cdot a\theta_0\nabla\Delta\theta \approx (q/4\pi\varepsilon_0(1-\beta)^2 a^2\theta_0)\Delta\dot{\Theta}, \qquad (4.15)$$

$$\boldsymbol{E}\cdot a\theta_0\nabla\theta_0 \approx (q/4\pi\varepsilon_0(1-\beta)^2 a^2\theta_0)\dot{\Theta}_0, \qquad (4.16)$$

$$\boldsymbol{E}\cdot\nabla z \approx (q/4\pi\varepsilon_0(1-\beta)^2 a^2\theta_0)\dot{Z}, \qquad (4.17)$$

where the three universal similarity functions are defined by

$$\Delta\dot{\Theta}(\Delta X, Z) = \left(1 + \frac{1}{2}\,\Delta\Theta^2 - \frac{1}{2}\,Z^2\right) \Big/ \left(1 + \frac{1}{2}\,\Delta\Theta^2 + \frac{1}{2}\,Z^2\right)^3, \qquad (4.18)$$

$$\dot{\Theta}_0(\Delta X, Z) = \left(1 - \frac{1}{2}\,\Delta\Theta^2 + \frac{1}{2}\,Z^2\right) \Big/ \left(1 + \frac{1}{2}\,\Delta\Theta^2 + \frac{1}{2}\,Z^2\right)^3, \qquad (4.19)$$

$$\dot{Z}(\Delta X, Z) = Z\Delta\Theta \Big/ \left(1 + \frac{1}{2}\,\Delta\Theta^2 + \frac{1}{2}\,Z^2\right)^3. \qquad (4.20)$$

Here, $\Delta\Theta = [\cdot]^{1/3} - 2(1 + \frac{1}{2}Z^2)[\cdot]^{-1/3}$, where $[\cdot] = \left[3\Delta X + \sqrt{8(1 + \frac{1}{2}Z^2)^3 + 9\Delta X^2}\right]$, the square and cube roots being real and positive, and ΔX and Z are defined by

$$\Delta X = \Delta x/a(1-\beta)^{3/2}, \quad Z = z/a\theta_0(1-\beta)^{1/2}, \qquad (4.21)$$

with $\Delta x = x - x_0$ and $x_0 = -a\theta_0 + \sqrt{(a\theta_0/\beta)^2 - z^2}$. (Also $\Delta\Theta$ represents $\Delta\theta/(1-\beta)^{1/2}$ and Θ_0 represents $\theta_0/(1-\beta)^{1/2}$ but, as intermediate variables, these are not strictly part of the specification.)

5. Field lines

The field lines or 'integral curves' of the 'flow' equations (4.18–4.20) can be found analytically (below). The first and last equations are the primary ones, since the right-hand sides of all three equations depend on $\Delta\Theta$ and Z only. They preserve invariant the quantity $Z_I \equiv (1 + \frac{1}{2}\Delta\Theta^2 + \frac{1}{2}Z^2)/Z$, meaning that the vector $(\Delta\dot{\Theta}, \dot{Z})$ is tangent to the contours of this quantity. These contours are the nested circles of 'bipolar' coordinates (otherwise known as 'coaxal' or 'coaxial' circles), with Z_I being the coordinate of its circle's centre along the Z axis. The circle's radius is $\sqrt{Z_I^2 - 2}$, with zero radius circles at $Z = \pm\sqrt{2}$. Nested bipolar circles are realized elsewhere in physics as magnetic field lines of parallel wires with opposite currents, or in geometry as the stereographic projection of latitude lines projected from a equator point rather than a pole.

The field lines, then, lie on twin nests of bipolar cylinders of circular cross-section in $\Delta\Theta$, Z coordinates (figure 5). They wind around their cylinders in distorted helices. To specify them introduce a coordinate Φ which measures angle around the circles from the point nearest the orbit plane (increasing initially in the direction of increasing x). Then, in terms of this parameter, and of the cylinder centre coordinate Z_I:
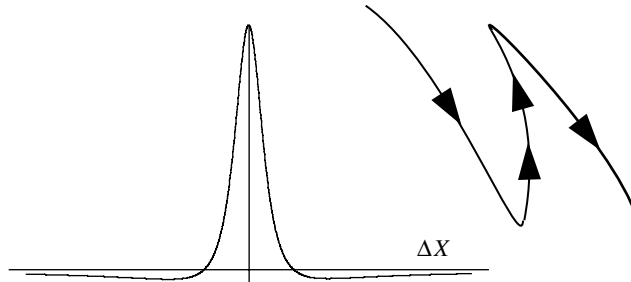
Figure 4. The peak electric field of synchrotron radiation. The field is largest in the orbit plane, near, and in a direction parallel to, the unwrap spiral. It has a universal similarity form supplied in full in equations (4.15–4.21). In this plot, the component of the field in the spiral direction is shown as a function of scaled coordinate ΔX ($\propto distance \times \gamma^3$) across the spiral in the orbit plane $z=0$. The universal function shown is $(1-\frac{1}{2}\Delta\Theta^2)/(1+\frac{1}{2}\Delta\Theta^2)^3$ with $\Delta\Theta = [\cdot]^{1/3} - 2[\cdot]^{-1/3}$, where (deriving from equations (4.9) or (4.19)). The peak field strength is proportional to γ^4. The corresponding electric field line has the zig-zag form sketched, with the two turning points being the two zeros of the plotted field component, and the field being much stronger in between them than outside.

$$\Delta\Theta = \sqrt{Z_I^2 - 2} \, \sin\Phi, \qquad (5.1)$$

$$\Theta_0 = 2\sqrt{2} \tan^{-1}\left[\frac{1}{\sqrt{2}}\left(Z_I + \sqrt{Z_I^2 - 2}\right)\tan\frac{\Phi}{2}\right] - \sqrt{Z_I^2 - 2}\,\sin\Phi + \text{const.}, \quad (5.2)$$

$$Z = Z_I - \sqrt{Z_I^2 - 2}\,\cos\Phi, \qquad (5.3)$$

where different values of the constant in the second equation label different field lines on the cylinder (translates of each other along the cylinder). All lines on all cylinders have the *same* physical repeat distance $2\sqrt{2}\pi a\theta_0\sqrt{1-\beta}$ along the cylinder (corresponding to a repeat in Θ_0 of $2\sqrt{2}\pi$).

As figure 5 shows, on narrow cylinders the field line helices are little distorted. On cylinders of radius greater than $\sqrt{6}$, which are wide enough to cross the hyperbolas $1 - \frac{1}{2}\Delta\Theta^2 + \frac{1}{2}\Delta Z^2 = 0$, the lines backtrack along the cylinder temporarily in the region where $1 - \frac{1}{2}\Delta\Theta^2 + \frac{1}{2}Z^2 < 0$ while still winding around it azimuthally. As can be seen from the picture, and anticipated from the equations, for large radius cylinders the field lines have a planar circular shape for most of their path around the cylinder, and then a skip to the next such circle. These circle arcs in $\Delta\Theta$, Θ_0, Z space actually map, very nearly, to arcs of circles in true space. Indeed, they are the circle field lines mentioned near the beginning above, not too close to the high-field region. That is, they correspond to the larger arcs of circles between U_1 and U_2 in figure 3, rather than the smaller ones through the high-field region. Of course, very far away from the high-field region our field lines, which involve the cubic approximation (4.2), cannot expect to reproduce the true field line circles accurately.
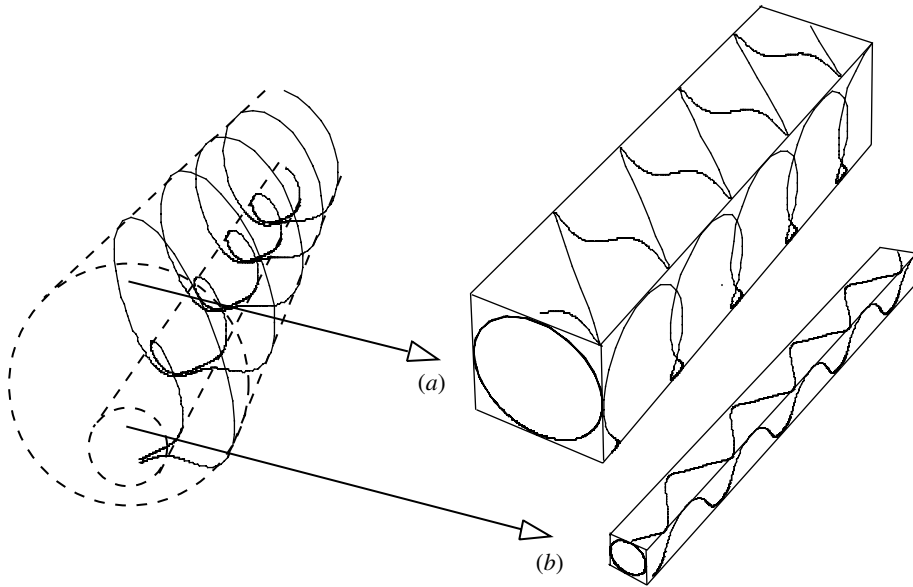
Figure 5. Windings of electric field on two selected bipolar cylinders in the scaled coordinates ($\Delta\Theta$, Z). Depicted are two field lines flowing into the page, with their shapes more clearly seen in top and side view projections. At smaller radii (*b*) the field lines form slightly distorted helices, while at larger radii (*a*) they form stacked circle arcs with short linking sections. All the field lines have the same repeat distance proportional to $1/\gamma$. This picture would have an exact mirror image by reflection in the orbital plane.

6. Concluding remarks

– It is interesting to check the flux of electric field, the correct value q/ε_0, for any surface enclosing the charge, being known from Gauss' law. A preliminary remark is that for particular surfaces, namely the spheres of constant retardation, the flux through the surface comes entirely from $\boldsymbol{E}_{\mathrm{vel}}$, since $\boldsymbol{E}_{\mathrm{acc}}$ is tangential. However, this does not apply to other surfaces because neither $\nabla\cdot\boldsymbol{E}_{\mathrm{acc}}$ nor $\nabla\cdot\boldsymbol{E}_{\mathrm{vel}}$ is individually zero, only their sum is. In the relativistic limit $\boldsymbol{E}_{\mathrm{vel}}$ vanishes except near the unwrap spiral, and, therefore, $\nabla\cdot\boldsymbol{E}_{\mathrm{acc}}$ must vanish except in the neighbourhood of the spiral, which therefore, controls the flux. It is straightforward to evaluate the flux through a cross-section half plane. It is the integral over the plane of $\boldsymbol{E}\cdot a\theta_0\nabla\theta_0$ in equation (4.15):

$$(q/4\pi\varepsilon_0(1-\beta)^2 a^2\theta_0)\iint \frac{(1-\frac{1}{2}\Delta\Theta^2+\frac{1}{2}Z^2)}{(1+\frac{1}{2}\Delta\Theta^2+\frac{1}{2}Z^2)^3}\,\mathrm{d}z\mathrm{d}x. \tag{6.1}$$

The Jacobian for conversion to $\mathrm{d}\Delta\Theta\mathrm{d}Z$ is $(\partial\Delta x/\partial\Delta\Theta)(\partial z/\partial Z)$ (since $(\partial z/\partial\Delta\Theta)=0$), which is found from equation (4.2), and the definition of Z. This gives the Jacobian as $(1-\beta)^2 a^2\theta_0(1+\frac{1}{2}+\Delta\Theta^2+\frac{1}{2}Z^2)$. The integral is marginally convergent and gives the correct value q/ε_0, provided the $\Delta\Theta$ integration is performed last (otherwise it gives zero, or half the result if performed in polar coordinates). We have not sought justification for the

favourable order of integration which probably requires more than just the present, dominant, asymptotics.

– A limitation of the formulas should be mentioned. They are not valid very close to the charge, where the short distance limit competes with the relativistic one. Thus, within a distance of $\sim a/\gamma^2$ the velocity field $\boldsymbol{E}_{\text{vel}}$ becomes significant (even dominant) over $\boldsymbol{E}_{\text{acc}}$, and also the cubic approximation is insufficient.

– The field formulas have more general applicability than to uniform motion in a circle. By Lorentz transformation of the specified field with a uniform motion perpendicular to the orbit plane, the field of a charge in helical motion due to an external uniform magnetic field can be accessed, for example.

More speculatively, further extension of the formalism to general highly relativistic motion may be possible as follows. For any charge trajectory with a present position Q, space is again filled with nested spheres of constant retardation, centres R. For each there is a centre of curvature O of the motion, an extrapolated position S and peak field point T (with $\text{RT}=\text{RS}/\beta$ as before). It may be that any longitudinal acceleration along the path, or torsion of the curve (in the sense of Frenet), do not affect the field to leading order. Then, in the cross-section half plane, the field should be given by the stated formulas.

– The magnetic field as opposed to the electric deserves comment. It is much simpler in that, by equation (3.4), it is exactly tangent to the retardation spheres. In consequence the lines of magnetic field are exactly closed loops (having zero divergence and lying in surfaces implies loops). Relativistically, the loops are everywhere orthogonal to the circle field lines of the field $\boldsymbol{E}_{\text{acc}}$, that is, they are themselves nests of circles on the retardation spheres, enclosing the points U_1 and U_2. Only the smallest loops near these points (where $\boldsymbol{E}_{\text{vel}}$ dominates $\boldsymbol{E}_{\text{acc}}$) are distorted. The sense of circulation is such that the B at the symmetry point T is antiparallel to the angular velocity vector of the charge circulation. (Together the orthogonal circles of $\boldsymbol{E}_{\text{acc}}$ and $\boldsymbol{B}$ form a Möbius transform of the latitude-longitude mesh.) When displayed in the cross-section scaled space, $\Delta\Theta$, Z the magnetic flow is around a set of bipolar circles (since, circles in Θ_0, Z on the retardation sphere become circles in $\Delta\Theta$, Z). In fact, the magnetic family of bipolar circles is identical to the electric family rotated by a right angle. The zero size circles lie at the two points $\Delta\Theta = \pm\sqrt{2}$, Z$=0$, mentioned after equation (4.9) above. The magnetic field lines in $\Delta\Theta$, Θ_0, Z are just 45° cuts ($\mathrm{d}\Delta\Theta/\mathrm{d}\Theta_0 = -1$, since Θ is constant) across the magnetic bipolar cylinders.

– Analysis of the high fields from a hypothetical point source circulating faster than light (as a Green function for a superluminal wave of charge or current density) has been supplied in papers by H. Ardavan. These are cited, with the necessary correction of principle, in Hannay (submitted). There exist infinitely strong fields (on caustic surfaces) for any $\beta > 1$, quite different from the strong fields analysed here which only approach infinity in the limit as $\beta \to 1$ from below.

References

Duke, P. J. 2000 *Synchrotron radiation.* Oxford: Oxford University Press.

Hannay, J. H. Submitted. Comment on spectral and polarization characteristics of the nonspherically decaying radiation generated by polarization currents with superluminally rotating distribution patterns.

Jackson, J. D. 1999 *Classical electrodynamics*, 3rd edn. New York: Wiley.

Risley, J. S., McPherson, A. & Westerveld, W. B. 1981 Use of a scaling relationship for synchrotron radiation. *Phys. Rev. A* **24**, 3255–3260. (doi:10.1103/PhysRevA.24.3255.)

Tsien, R. Y. 1972 Pictures of dynamic electric fields. *Am. J. Phys.* **40**, 46–57.